

# Quadratic Element Integration of Approximated First Order Polarization Tensor for Sphere.

Suzarina Ahmed Sukri <sup>a</sup>, Yeak Su Hoe <sup>a,\*</sup>, Taufiq Khairi Ahmad Khairuddin <sup>a, b</sup>.

<sup>a</sup> Department of Mathematical Sciences, Faculty of Science, Universiti Teknologi Malaysia, 81310 UTM Johor Bahru, Johor, Malaysia

<sup>b</sup> UTM Centre for Industrial and Applied Mathematics (UTM-CIAM), Universiti Teknologi Malaysia, 81310 UTM Johor Bahru, Johor, Malaysia

\* Corresponding author: s.h.yeak@utm.my

## Article history

Received 29 Mar 2020  
 Revised 14 May 2020  
 Accepted 30 August 2020  
 Published Online 20 October 2020

## Abstract

Polarization tensor is an object-specific property in order to indicate its shape, size and also the material used. In this paper, we describe an accurate and easy-implemented method based on numerical integration in order to compute the first order polarization tensor. We proposed an alternative method to deal with boundary integral equation of first order polarization tensor which is quadratic element numerical integration. This method uses standard three points Gaussian quadrature in order to generate the singular integral operator matrix of polarization tensor. Different values of object's conductivity are used in order to study the behavior of the polarization tensor. The validation of the results is based on the exact solution provided for sphere and ellipsoid geometry by previous researcher. Moreover, numerical computation showed that the quadratic element integration generates high accuracy numerical results for the approximated first order polarization tensor. The numerical results are illustrated in graphical form in order to show the validity of the proposed scheme.

**Keywords:** Quadratic element integration; polarization tensor; boundary integral equation; Gaussian quadrature; mesh

© 2020 Penerbit UTM Press. All rights reserved

## INTRODUCTION

Recently, the study of polarization tensor (PT) have attracted the attention of researchers interested in science and engineering area. The perturbation due to the presence of conducting object inclusion can be represented by asymptotic formula and the dominant terms of the formula is said to be the PT [1–3]. The term PT first arose from the study of Polya [4] where he defined PT as virtual mass involving the motion of solids through fluid when the solids have zero conductivity. This study has then been extensively developed by researchers as in [5,6] where they denoted the new PT as Polya-Szego PT. Later, in recent years, the term Generalized Polarization Tensor (GPT) which combines the infinite numbers of PT, has been defined and the lowest order of GPT is said to be first order PT (FPT) [1]. FPT is a rank 2 GPT where it contains geometric and physical properties of an object inclusion. The information about the object is beneficial to determine between used and unused material underground for example. The concept of GPT has generalized the old concept of Polya-Szego PT that has been studied by a number of researchers in various areas such as in [1,7–9]. Not only that, the applications of PT can be seen through various applications in metal detection which is landmine detection [10–15], electrosensing fish [16–22] and also in dilute composites models.

Several numerical methods have been implemented by former researchers in order to compute the first order PT [23,24]. For example, semi algebraic method has been employed by Capdeboscq *et al.* where they have shown that, the computation of objects with higher conductivity would produce lower convergence of PT compared to lower conductivity object [24]. Unfortunately, the method that has been

derived is restricted and can only be applied to two dimensional cases of PT. Then, from this, the study of computational PT has been extended by a few researchers where they adopt different numerical methods such as boundary element method (BEM) and also linear element integration [17,25,26]. New technique has been introduced where the operating system regime called BEM++ in order to compute first order of PT is used [25]. Ammari and Kang [1] defined PT in the form of boundary integral equation where from this boundary integral, Khairuddin and Lionheart [17] used linear element integration in order to numerically calculate PT for various kinds of shapes of object such as sphere, cylinder, cube and the other basic symmetrical shapes. Their study is can be used for any three dimensional domains.

Hence from the numerical methods that has been introduced and developed, we came out with new technique to numerically calculate the FPT which is using quadratic element numerical integration. Here, our method is slightly different from the method of Khairuddin and Lionheart [17] where we compute the boundary integral equation with the usage of Gaussian quadrature of three points and six nodal shape functions involving  $\xi$  and  $\eta$ . The shape function of  $\xi$  and  $\eta$  is used in order to change the local coordinates to global coordinates. Firstly, we are going to review the definition of PT in the form of boundary integral equation, and then we will provide the methodology using quadratic interpolation. The comparison between analytical solution (provided in [1]) with numerical solution of quadratic element integration were made and the convergence of the results will be analysed. Not even that, we will also compare the numerical solution for first order PT by using linear element numerical integration with our approach.

For next section will review the mathematical background of PT that will help to increase the understanding of PT.

**FIRST ORDER POLARIZATION TENSOR**

The terminology of PT is originated from the transmission problem and has been defined by the author in [1]. Consider a Lipschitz bounded domain of  $B$  in such that the origin,  $O$  is inside  $B$ . Then, Ammari and Kang stated the condition of the conductivity which denoted as  $k$  must not be equal to 1 and is between 0 to  $+\infty$  ( $0 < k \neq 1 < \infty$ ). Let  $u$  be the solution of the following transmission problem where  $H$  is the harmonic function in  $\mathbb{R}^3$

$$(u - H)(x) = \sum_{|i|,|j|=1}^{+\infty} \frac{(-1)^{|i|}}{i!j!} \partial_x^i \Gamma(x) M_{ij}(k, B) \partial^j H(0) \text{ as } |x| \rightarrow +\infty. \quad (1)$$

Here,  $i = (i_1, i_2, i_3)$  and  $j = (j_1, j_2, j_3)$  are the multi indices,  $\Gamma$  is the fundamental solution of the Laplacian while  $\widehat{M}_{ij}$  is the GPT. The definition of GPT is expressed as an integral equation over the boundary domain of  $B$  as stated in equation (2)

$$\widehat{M}_{ij} = \int_{\partial B} y^j \phi_i(y) d\sigma(y), \quad y \in \partial B \quad (2)$$

$y_j$  is the coordinates for element  $y$  while  $\phi_i(y)$  is defined as linear system of equations as in equation (3)

$$\phi_i(y) = (\lambda I - K_B^*)(v_x \cdot \nabla x^i)(y) \quad y \in \partial B \quad (3)$$

for  $x, y$  inside the domain  $B$  with  $\lambda = (k + 1)/(2k - 2)$ . The singular integral operator is defined with Cauchy principle value  $P.V.$  where

$$K_B^* \phi(x) = \frac{1}{4\pi} P.V. \int_{\partial B} \frac{\langle x - y, v_x \rangle}{|x - y|^3} \phi(y) d\sigma(y) \quad (4)$$

for  $\phi(x) \in L^2(\partial B)$  such that  $L^2(\partial B)$  is the space of square integrable functions on  $\partial B$ . Throughout this study, our main intention in order to find PT is by solving the equation in (2), (3) and (4). The only parameter that we need to consider in order to estimate the first order of PT is the conductivity and also the shape of the object inclusion  $B$ . We also will refer to the properties of PT that is proven by Ammari and Kang [1] in order to validate the numerical results.

**Theorem 1.** *If  $k > 1$ , then the first order PT is a positive definite(matrix) while it is a negative definite matrix if  $0 < k < 1$ .*

For the next section, we are going to review the analytical solution that has been provided by previous researchers.

**Analytical Solution of First Order Polarization Tensor**

The analytical solution of PT has been derived initially which is based on the geometry of ellipsoid [1]. The authors consider the ellipsoid  $x^2/a + y^2/b + z^2/c = 1$  with semi principle axes  $a, b$  and  $c$  where  $0 < c < b = a$ . This analytical solution is represented in the form of matrix 3 by 3 where the main diagonal is in the form of integral containing the semi principle axes of  $a, b$  and  $c$ . The following matrix represents the first order PT of object  $B$  with specific conductivity

$$\widehat{M}(k, B) = (k - 1)|B| \begin{bmatrix} \frac{1}{(1 - d_1) + kd_1} & 0 & 0 \\ 0 & \frac{1}{(1 - d_2) + kd_2} & 0 \\ 0 & 0 & \frac{1}{(1 - d_3) + kd_3} \end{bmatrix} \quad (5)$$

where  $|B|$  is referred as the volume of an object while  $d_1, d_2, d_3$  are in the form of integral equation containing semi principle axes  $a, b, c$  as in equation (6).

$$\begin{aligned} d_1 &= \frac{bc}{a^2} \int_1^{+\infty} \frac{1}{t^2 \sqrt{t^2 - 1 + \left(\frac{b}{a}\right)^2} \sqrt{t^2 - 1 + \left(\frac{c}{a}\right)^2}} dt, \\ d_2 &= \frac{bc}{a^2} \int_1^{+\infty} \frac{1}{\left(t^2 - 1 + \left(\frac{b}{a}\right)^2\right)^{\frac{3}{2}} \sqrt{t^2 - 1 + \left(\frac{c}{a}\right)^2}} dt, \\ d_3 &= \frac{bc}{a^2} \int_1^{+\infty} \frac{1}{\sqrt{t^2 - 1 + \left(\frac{b}{a}\right)^2} \left(t^2 - 1 + \left(\frac{c}{a}\right)^2\right)^{\frac{3}{2}}} dt, \end{aligned} \quad (6)$$

By setting  $a = b = c$ , the integrals of  $d_1, d_2$  and  $d_3$  will resulted to 1/3 and the first order PT of sphere is given as

$$\widehat{M}_A(k, B) = (k - 1)|B| \begin{bmatrix} \frac{3}{2 + k} & 0 & 0 \\ 0 & \frac{3}{2 + k} & 0 \\ 0 & 0 & \frac{3}{2 + k} \end{bmatrix} \quad (7)$$

where in this case the volume of sphere,  $|B|$  will be equal to  $4/3\pi r^3$ . From the integral equation of PT in (2), we will implement the quadratic element integration technique and use the meshing software to discretize the domain  $B$ . Next part will describe the discretization of the geometry using the Netgen Mesh Generator software.

**Discretization of Object using Netgen Mesh Generator (NG Solver)**

Before we compute the first order PT using our approach, we must firstly discretize the object which is sphere into triangular mesh. This is crucial so that we can observe how the meshes sizes affect the accuracy of the computation of first order PT. Therefore, the adoption of Netgen mesh generator software is needed to perform triangularization to the specific object. This NG Solver is user-friendly software that can generate the mesh and also the nodal points of each triangular element [27]. It will auto-generate the meshes where it allows the user to choose linear element which involve three nodal points or quadratic triangular elements which involve six nodal points. The meshing option that build in NG Solver must be set to second order element which represent the quadratic interpolation involving six nodal points. Figure 1 shows sphere geometry that has been discretized into 968 triangular elements using NG Solver software.

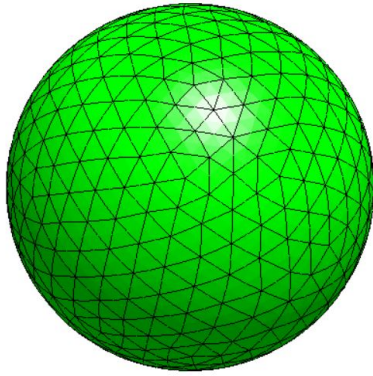


**Figure 1** The discretization of sphere  $x^2 + y^2 + z^2 = 1$  into 968 triangular elements using NG Solver software.

From this triangularization, we will import the information that has been generated by Netgen software into MATLAB routine. Then after that, we will start to compute the first order PT. Figure 2 show the process to discretize the geometry by NG Solver starting From meshing size to be equal to 68 triangles until 968 triangles.

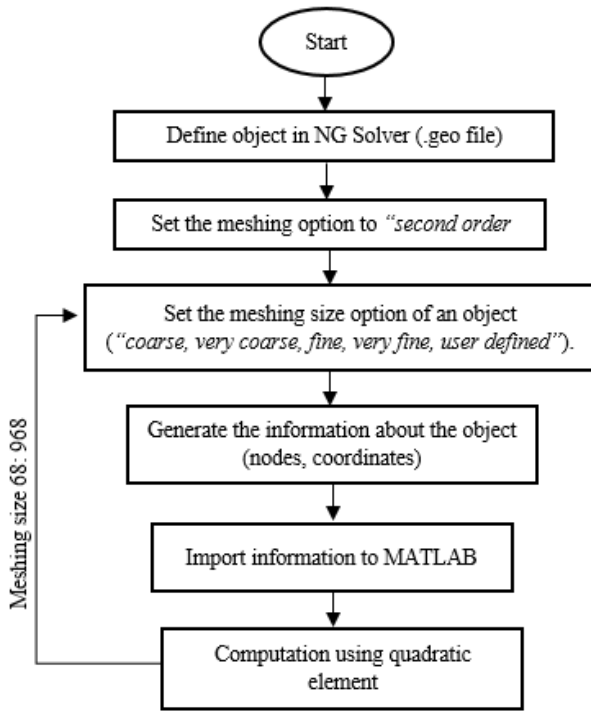


**Figure 2** Flow chart to show the process using NG Solver.

Next section provides the methodology of quadratic element numerical integration and the resulted matrix system after the implementation of the approach.

### QUADRATIC ELEMENT NUMERICAL INTEGRATION

Throughout this paper, we intend to implement numerical integration technique in order to solve the integral of PT. The computation of the integral of the first order PT involves the computation of the singular integral operator,  $K_B^*$ , solving linear system of  $\phi_i(y)$  and lastly, the integral of PT itself. We expressed the singular integral operator,  $K_B^*$  in form of integral equation containing surface projection and Jacobian as in the form

$$\begin{aligned}
 K_B^* \phi(x) &= \frac{1}{4\pi} P.V. \int_{\partial B} \frac{\langle x-y, v_x \rangle}{|x-y|^3} \phi(y) d\sigma(y), \\
 &= \frac{1}{4\pi} P.V. \int_{\partial B} \frac{\langle x-y, v_x \rangle}{|x-y|^3} \phi(y) \text{SurP}(\xi, \eta) |Jac(\xi, \eta)| d\xi d\eta(y).
 \end{aligned}
 \tag{8}$$

Here,  $x$  and  $y$  is the elements of object inclusion whilst  $x - y$  is the distance between both elements.  $v_x$  is the outward normal vector at element  $x$ ,  $\text{SurP}(\xi, \eta)$  is the surface projection of the triangular elements while  $Jac(\xi, \eta)$  is the Jacobian in the form of  $\xi$  and  $\eta$ . Since the analytical solution of sphere is provided, we use sphere geometry,  $x^2 + y^2 + z^2 = 1$  to compute its approximated first order polarization. The surface projection will yield to

$$\text{SurP} = \psi(x, y, z) = \frac{\langle 2x, 2y, 2z \rangle}{|\langle 2x, 2y, 2z \rangle|}
 \tag{9}$$

while

$$|Jac| = \begin{bmatrix} (4\xi - 1)x_1 + (-4\tau + 1)x_3 + 4\eta x_4 & (4\xi - 1)y_1 + (-4\tau + 1)y_3 + 4\eta y_4 \\ -4\eta x_5 + (4 - 8\xi - 4\eta)x_6 & -4\eta y_5 + (4 - 8\xi - 4\eta)y_6 \\ (4\eta - 1)x_2 + (-4\tau + 1)x_3 + 4\xi x_4 & (4\eta - 1)y_2 + (-4\tau + 1)y_3 + 4\xi y_4 \\ + (4 - 4\xi - 8\eta)x_5 - 4\xi x_6 & + (4 - 4\xi - 8\eta)y_5 - 4\xi y_6 \end{bmatrix}
 \tag{10}$$

Equation in (9) and (10) present the surface projection and the Jacobian that we are using throughout the study. We change the local coordinates into global coordinates by implementing the shape functions of six nodes as stated in equation (11).

$$\begin{aligned}
 x(\xi, \eta) &= \sum_{m=1}^6 x_m N_m(\xi, \eta), \\
 y(\xi, \eta) &= \sum_{n=1}^6 y_n N_n(\xi, \eta), \\
 z(\xi, \eta) &= \sum_{l=1}^6 z_l N_l(\xi, \eta).
 \end{aligned}
 \tag{11}$$

where  $N_m, N_n$  and  $N_l$  is the shape function for  $m = n = l = 1 \dots 6$  which indicate 1 until six nodal points of each triangular elements. They can be expressed as

$$\begin{aligned}
 N_1 &= 2\xi^2 - \xi, \\
 N_2 &= 2\eta^2 - \eta, \\
 N_3 &= 2\xi^2 + 2\eta^2 + 4\xi\eta - \xi - \eta + 1, \\
 N_4 &= 4\xi\eta, \\
 N_5 &= -4\eta^2 - 4\xi\eta + 4\eta, \\
 N_6 &= -4\xi^2 - 4\xi\eta + 4\xi.
 \end{aligned}
 \tag{12}$$

Instead of using the midpoint as in Khairuddin and Lionheart in [28], we are going to use the Gaussian points and weight in order to transform the local coordinates of the meshes that had been discretized into global coordinates containing  $\xi$  and  $\eta$ . The standard Gaussian quadrature of three points during the computation of first order PT are  $\xi = 2/3, \eta = 1/6$  (for Gauss points 1 denoted as  $GP^1$ ),  $\xi = 1/6, \eta = 2/3$  (for Gauss points denoted as 2 denoted as  $GP^2$ ) and lastly  $\xi = 1/6, \eta = 1/6$  (for Gauss points 3 denoted as  $GP^3$ ). The linear integration element integration that has been done by Khairuddin and Lionheart [23] produced  $N \times N$  matrix system of  $K_B^*$ . We denoted the Gaussian point for element  $x$  by  $GP_{e_x}$  while for element  $y$  we denoted as  $GP_{e_y}$ . For our case, we will obtain  $3N \times 3N$  matrix system as in the form

$$(GP_{e_x}, GP_{e_y}) = \begin{pmatrix} (GP_{e=1}^1, GP_{e=1}^{(1...3)}) & \dots & (GP_{e=1}^1, GP_{e=N}^{(1...3)}) \\ (GP_{e=1}^2, GP_{e=1}^{(1...3)}) & \dots & (GP_{e=1}^2, GP_{e=N}^{(1...3)}) \\ (GP_{e=1}^3, GP_{e=1}^{(1...3)}) & \dots & (GP_{e=1}^3, GP_{e=N}^{(1...3)}) \\ \vdots & \ddots & \vdots \\ (GP_{e=N}^1, GP_{e=1}^{(1...3)}) & \dots & (GP_{e=N}^1, GP_{e=N}^{(1...3)}) \\ (GP_{e=N}^2, GP_{e=1}^{(1...3)}) & \dots & (GP_{e=N}^2, GP_{e=N}^{(1...3)}) \\ (GP_{e=N}^3, GP_{e=1}^{(1...3)}) & \dots & (GP_{e=N}^3, GP_{e=N}^{(1...3)}) \end{pmatrix}$$

which yield to matrix system of  $K_B^*$  given by

$$K_B^* \phi(X^*) = \begin{pmatrix} w_s K(x_1^1, y_1^{(1...3)}) & \dots & w_s K(x_1^1, y_N^{(1...3)}) \\ w_s K(x_1^2, y_1^{(1...3)}) & \dots & w_s K(x_1^2, y_N^{(1...3)}) \\ w_s K(x_1^3, y_1^{gp(s)}) & \dots & w_s K(x_1^3, y_N^{(1...3)}) \\ \vdots & \ddots & \vdots \\ w_s K(x_N^1, y_1^{(1...3)}) & \dots & w_s K(x_N^1, y_N^{(1...3)}) \\ w_s K(x_N^2, y_1^{(1...3)}) & \dots & w_s K(x_N^2, y_N^{(1...3)}) \\ w_s K(x_N^3, y_1^{(1...3)}) & \dots & w_s K(x_N^3, y_N^{(1...3)}) \end{pmatrix} \begin{pmatrix} \phi_{y_1}^1 \\ \phi_{y_1}^2 \\ \phi_{y_1}^3 \\ \vdots \\ \phi_{y_N}^1 \\ \phi_{y_N}^2 \\ \phi_{y_N}^3 \end{pmatrix} \quad (13)$$

Here, 1, 2 and 3 indicate the Gaussian points that we have used. After obtaining the matrix of  $K_B^*$ , we substitute this matrix into linear system of  $\phi_i(y)$ , which resulted to  $3N \times 3$  matrix. The method that we used in order to solve the linear system of  $\phi_i(y)$  is Gaussian elimination method (GEM). It is well known that in order to find the solution of matrix system, we simply need to find the inverse of  $(\lambda I - K_B^*)$  and then multiplying it with the outward normal vector of element  $x$ . Lastly, for the integral of PT,  $\hat{M}_{ij}$ , we implement the same technique as in the integral of  $K_B^*$  where the integral can be expressed as

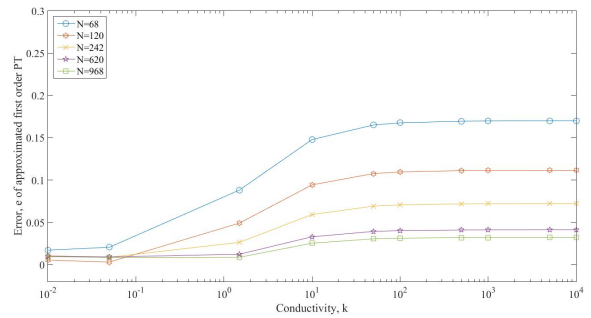
$$M_{ij} = \int_{\partial B} y^j \phi_i(y) \text{SurP}(\xi, \eta) dA(y) = \int_{\partial B} y^j \phi_i(y) \text{SurP}(\xi, \eta) |\text{Jac}(\xi, \eta)| \cdot d\xi d\eta(y) \quad (14)$$

which resulted to  $3 \times 3$  matrix. For the next section, we are going to apply this approach to numerically calculate the first order of PT for specific geometry which is sphere.

**NUMERICAL EXAMPLES**

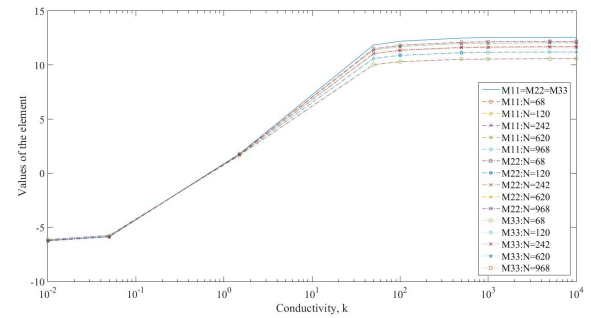
**Numerical comparison between analytical and approximated first order PT using quadratic element numerical integration**

The first order PT for the sphere with radius,  $r = 1$  is approximated with different number of meshes which are,  $N = 68, 120, 242, 620$  and  $968$  triangles. For that discretization, we used different times of meshing option in NG Solver which are moderate, fine, very fine, user defined and refinement. Figure 3 depicts the relative error,  $RE = \frac{\|\hat{M}_A - \hat{M}_E\|_2}{\|\hat{M}_A\|_2}$ , between the approximated first order PT,  $\hat{M}_E$  using quadratic element numerical integration with the analytical solution of PT,  $\hat{M}_A$ .



**Figure 3** The convergence of  $\frac{\|\hat{M}_A - \hat{M}_E\|_2}{\|\hat{M}_A\|_2}$  for approximated first order PT,  $\hat{M}_E$  for the sphere radius,  $r = 1$  with the analytical solution of first order PT,  $\hat{M}_A$  on the mesh with 68, 120, 242, 620 and 968 triangles against conductivity  $k$ .

Based on Figure 3, we can observe that, as  $N$  increases, the relative error approximated for the first order PT will decrease. However, the error,  $e$  is unbounded as the values of the conductivity increases ( $k \rightarrow +1$ ) regardless of the total number of surface elements used. When we used  $N = 120$ , at first, the error for the approximated PT showed the lowest error but it started to increase as the number of conductivity,  $k > 10$ . For the surface element of 968 meshes, the error showed less increment compared to other values of meshes. This indicates that the smaller meshes would produce less error compared to big mesh.



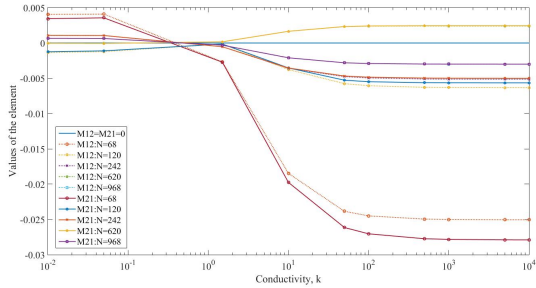
**Figure 4** The first, second and third main diagonal,  $\hat{M}_{11}, \hat{M}_{22}$  and  $\hat{M}_{33}$  of the approximated first order PT for sphere triangularized by 68, 120, 242, 620 and 968 triangles and the main diagonals for the analytical solution of first order PT.

Figure 4 showed the values of the elements for main diagonals  $\hat{M}_{11}, \hat{M}_{22}$  and  $\hat{M}_{33}$  as the conductivity increases. Here, the conductivity used are  $k = 0.01, 0.05, 1.5, 50, 100, 500, 1000, 5000$  and  $10000$ . For main diagonal,  $\hat{M}_{11}, \hat{M}_{22}$  and  $\hat{M}_{33}$ , since for analytical solution the computed result for those three diagonals share the same values, we plot the approximated first order PT for sphere in the same graphs. We can see from Figure 4 that the numerical solutions for  $\hat{M}_{11}, \hat{M}_{22}$  and  $\hat{M}_{33}$  for surface element 968 triangles showed very accurate values of the elements compared to other surface elements. This result satisfies the theorem that has been mentioned in previous section, where we can observe that, when the conductivity is less than 1 the first order PT is negative definite matrix. When the conductivity increases to more than 1, the matrix of the first order PT will be positive definite. Hence, from the theorem, we can conclude that, our approach is suitable and can be implemented in order to evaluate the matrix of first order PT.

On the other hand, non-diagonal for the approximated first order PT can be seen in Figure 5, 6 and 7 where, in Figure 5, the values for non-diagonal elements of  $\hat{M}_{12}$  and  $\hat{M}_{21}$  are depicted. At  $k = 1.5$  ( $k > 1$ ), the values of approximated first order PT become closer to 0. However, note that as we increased the conductivity  $k \rightarrow +\infty$ , the approximate values of first order PT is slowly diverge from its analytical solution. As for surface element  $N = 68$ , the values of approximated first order PT show less accurate results compared to other values of surface elements. This suggest that the usage of higher

number of surface elements is important so that we obtained an accurate approximation of PT.

For  $\hat{M}_{31}$  and  $\hat{M}_{13}$ , when we used surface element of 120, the values of approximated first order PT would diverge from its analytical solution. But for other values of surface elements, the non-diagonals are smaller and become closer to 0 as required by the analytical solution in equation (7). Moreover, an accurate values of element is shown as we computed non-diagonals of  $\hat{M}_{32}$  and  $\hat{M}_{23}$ . From Figure 7, the values of elements of approximated first order PT converge to 0 except for approximated first order PT for surface element of 68.



**Figure 5** The first non-diagonal,  $\hat{M}_{12}$  and  $\hat{M}_{21}$  of the approximated first order PT for sphere triangularized by 68,120,242,620 and 968 triangles and the non diagonals of the analytical solution of first order PT.

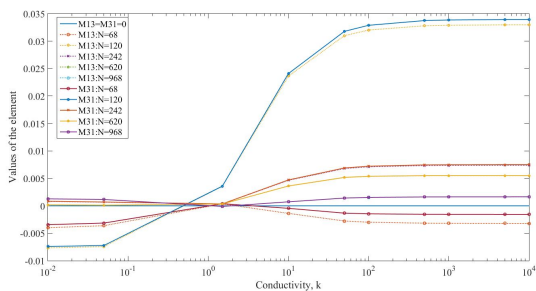


**Figure 6** The second non-diagonal,  $\hat{M}_{31}$  and  $\hat{M}_{13}$  of the approximated first order PT for sphere triangularized by 68,120,242,620 and 968 triangles and the non diagonals of the analytical solution of first order PT.

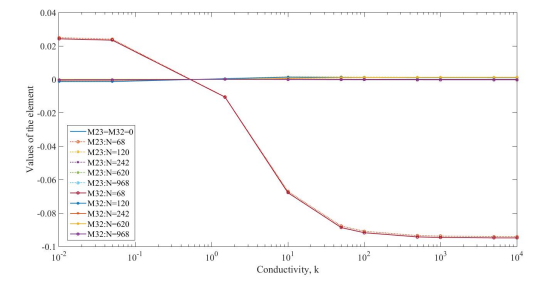


**Figure 7** The third non-diagonal,  $\hat{M}_{32}$  and  $\hat{M}_{23}$  of the approximated first order PT for sphere triangularized by 68, 120, 242, 620 and 968 triangles and the diagonals of the analytical solution of first order PT.

**Numerical comparison between first order PT using linear and quadratic element numerical integration**

In this section, comparison between approximated first order PT using linear and quadratic element will be computed and compared. We used different values of surface element,  $N$  in order to observe the convergence of approximated first order PT of both approach. By using sphere with radius,  $r = 0.01$  and fixing the conductivity of object to  $k = 1.5$ , we then will obtain the analytical solution as

$$\hat{M}_A = 10^{-5} \times \begin{bmatrix} 0.17952 & 0 & 0 \\ 0 & 0.17952 & 0 \\ 0 & 0 & 0.17952 \end{bmatrix} \quad (15)$$

By using linear element with 9920 surface elements, we can see that the matrix of first order PT become as follow

$$\hat{M}_L = 10^{-5} \times \begin{bmatrix} 0.17890 & 0 & 0 \\ 0 & 0.17890 & 0 \\ 0 & 0 & 0.17890 \end{bmatrix}, \quad (16)$$

while first order PT obtained by using quadratic element numerical integration yield to

$$\hat{M}_Q = 10^{-5} \times \begin{bmatrix} 0.17922 & 0 & 0 \\ 0 & 0.17922 & 0 \\ 0 & 0 & 0.17922 \end{bmatrix}. \quad (17)$$

From the matrix system in (15), (16) and (17), we can observed that, the numerical approximation of first order PT using quadratic interpolation,  $\hat{M}_Q$  is more accurate than linear element numerical integration,  $\hat{M}_L$ . The main diagonal will converge to positive definite matrix (since we use conductivity,  $k > 1$ ) for both approaches agrees with Theorem 1 that has been proven by Ammari and Kang [1]. However, the main diagonal for quadratic element showed better accuracy in term of approximation since the difference between main diagonal of analytical solution with the approach is 0.0003 while for linear element numerical integration is 0.0006. Since linear element integration is accurate only for planar triangle, therefore, it resulted to higher error in the approximation of first order PT than quadratic element.

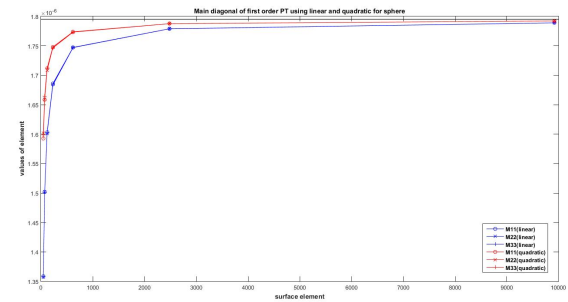


**Fig 8.** The first, second and third main diagonal,  $\hat{M}_{11}$ ,  $\hat{M}_{22}$  and  $\hat{M}_{33}$  of the approximated first order PT for sphere triangularized by 44, 72, 118, 230, 620, 2480 and 9920 triangles using linear and quadratic element numerical integration with its analytical solution.

Next, we constructed the graph of the first order PT using both approaches with different values of surface element in order to observe the accuracy and the convergence of the computed numerical results. Figure 8 depicted the main diagonal for approximated first order PT using different values of surface elements which are 44, 72, 118, 230, 620, 2480 and 9920 triangles. The straight line that shown in the graph is the analytical solution of first order PT of sphere with radius 0.01 and conductivity,  $k = 1.5$  as stated in matrix in (15). From the graph in Figure 8, we can see that, as we increases the surface elements from 44 to 9920 triangles, main diagonal for both approaches eventually lead to the analytical solution. However, we can see that the numerical approximation of first order PT of quadratic element is more closer than by using linear element numerical integration.

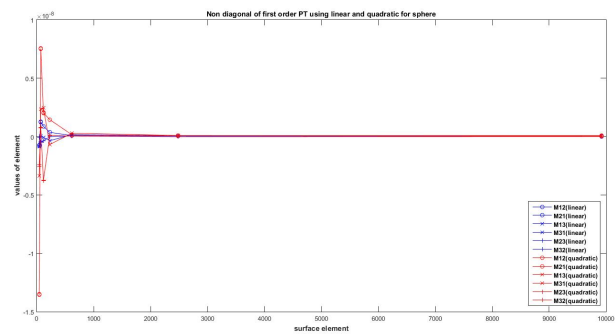


**Figure 9** The non-diagonal,  $\hat{M}_{12}$ ,  $\hat{M}_{13}$ ,  $\hat{M}_{21}$ ,  $\hat{M}_{23}$ ,  $\hat{M}_{31}$  and  $\hat{M}_{32}$  of the approximated first order PT for sphere triangularized by 44, 72, 118, 230, 620, 2480 and 9920 triangles using linear and quadratic element numerical integration with its analytical solution.

For values of non diagonal, both approximation of first order PT using linear and quadratic will eventually lead to 0 as shown in Figure 9. Non diagonal elements will converge to 0 especially when the surface element is set to finer mesh and it start converge to 0 when the meshes is at approximately 1000 triangles. At first, for both approaches, the approximated first order PT in not accurately computed especially when the surface element is 44.

This suggest that, for both main and non diagonal of approximated first order PT, the numerical results is very accurate at finer meshes compared to coarse meshes. Other than that, quadratic element numerical integration which involve six nodal points of triangles is efficient in order to numerically approximate the geometry containing curvy part as sphere rather than linear element which uses only three nodal points. Next section provide the discussion and conclusion that can be made from all the results obtained.

## DISCUSSION AND CONCLUSION

In this paper, we have shown that, the polarization tensor of rank 2 can be obtained more accurately by using our proposed method. The quadratic element numerical integration of Gaussian quadrature which involve six nodal points has been implemented to the transmission problem of PT in the form of boundary integral equation. We have included numerical results to illustrate how the tensors can be computed accurately by using quadratic element numerical integration by comparing it with the analytical results involving sphere provided by Ammari and Kang [1].

Not even that, we also provide the numerical comparison for our approach with the approach that has been used by Khairuddin and Lionheart [28]. These results indicate that, for a specific geometry, the convergence of the computed tensor can be achieved by using finer mesh instead of coarse mesh which can be generated by Netgen mesh generator. Not even that, we also have proven that, the approximation of first order PT using quadratic element numerical integration provide better convergence and higher in terms of their accuracy compared to linear element numerical integration.

The understanding and establishment of the study of PT is very crucial so that it can be applied to real life problem especially in science and engineering problem. Therefore, in future work, we intend to apply our approach to different range of objects and the numerical predictions of those objects will be computed.

## ACKNOWLEDGEMENT

The authors would like to express gratitude to the Ministry of Higher Education (MOHE) for their financial support through MyBrainSc scholarship during this study is conducted.

## REFERENCES

[1] Ammari, H., Kang, H. Polarization and Moment Tensors With Applications to Inverse Problems and Effective Medium Theory. vol. 162. Springer; 2007.

[2] Ammari, H., Vogelius, M. S., Volkov, D. Asymptotic formulas for perturbations in the electromagnetic fields due to the presence of inhomogeneities of small diameter II. the full Maxwell equations. *J. Des. Math. Pures. Appl.* 2001;80:769–814.

[3] Ammari, H., Chen, J., Chen, Z., Garnier, J., Volkov, D. Target detection and characterization from electromagnetic induction data. *J. Math. Pures. Appl.* 2014;101:54–75.

[4] Polyá, G. A minimum problem about the motion of a solid through a fluid.

*Proc. Natl. Acad. Sci.* 1947;33:218–21.

[5] Schiffer, M., Szego, G. Virtual Mass and Polarization. *Trans. Am. Math. Soc.* 1949;67:130–205.

[6] Polyá, G., Szego, G. Isoperimetric inequalities in mathematical physics. *B. Am. MathSoc.* 1953;59:588–602.

[7] Friedman, A., Vogelius, M. Identification of small inhomogeneities of extreme conductivity by boundary measurements: a theorem on continuous dependence. *Arch. Ration. Mech. Anal.* 1989;105:299–326.

[8] Jong, W. D., Cremer, F., Schutte, K., Storm, J. Usage of polarisation features of landmines for improved automatic detection. *Int. Soc. Opt. Photonics* 2000;4038:241–53.

[9] Ammari, H., Kang, H. Properties of the generalized polarization tensors. *Multiscale Model Simul.* 2003;1:335–48.

[10] Marsh, L. A., Ktistis, C., Järvi, A., Armitage, D. W., Peyton, A. J. Determination of the magnetic polarizability tensor and three dimensional object location for multiple objects using a walk-through metal detector. *Meas. Sci. Technol.* 2014;25:055107.

[11] Makkonen, J., Marsh, L. A., Vihonen, J., Järvi, A., Armitage, D. W., Visa, A., et al. KNN classification of metallic targets using the magnetic polarizability tensor. *Meas. Sci. Technol.* 2014;25:055105.

[12] Marsh, L. A., Ktistis, C., Järvi, A., Armitage, D. W., Peyton, A. J. Three-dimensional object location and inversion of the magnetic polarizability tensor at a single frequency using a walk-through metal detector. *Meas. Sci. Technol.* 2013;24:045102.

[13] Dekdouk, B., Marsh, L. A., Armitage, D. W., Peyton, A. J. Estimating Magnetic Polarizability Tensor of Buried Metallic Targets for Land Mine Clearance. *Springer* 2014:425–32.

[14] Dekdouk, B., Ktistis, C., Marsh, L. A., Armitage, D. W., Peyton, A. J. Towards metal detection and identification for humanitarian demining using magnetic polarizability tensor spectroscopy. *Meas. Sci. Technol.* 2015;26:115501.

[15] Abdel-rehim, O. A., Davidson, J. L., Marsh, L. A., Toole, M. D. O., Peyton, A. J. Magnetic polarizability tensor spectroscopy for low metal anti-personnel mine surrogates. *IEEE Sens. J.* 2016;16:3775–83.

[16] Von, D. E. G., Fetz, S. Distance, shape and more: Recognition of object features during active electrolocation in a weakly electric fish. *J. Exp. Biol.* 2007;210:3082–95.

[17] Khairuddin, T. K. A., Lionheart, W. R. B. Characterization of objects by electrosensing fish based on the first order polarization tensor. *Bioinspiration and Biomimetics* 2016;11:1–8.

[18] Hairuddin, T. K. A., Lionheart, W. R. B. Does electro-sensing fish use the first order polarization tensor for object characterization? Object discrimination test. *Sains Malaysiana* 2014;43:1775–9.

[19] Ammari, H. Modeling active electrolocation in weakly electric fish. *SIAM J. Imaging Sci.* 2013;6:285–321.

[20] Ammari, H., Boulier, T., Garnier, J., Wang, H. Shape recognition and classification in electro-sensing. *Proc. Natl. Acad. Sci.* 2014;111:11652–11657.

[21] Khairi, T., Lionheart, W. R. B. Polarization Tensor : Between Biology and Engineering. *Malaysian J M.ath. Sci* 2016;10:179–91.

[22] Ammari, H., Boulier, T., Garnier, J., Wang, H. Mathematical modelling of the electric sense of fish: The role of multi-frequency measurements and movement. *Bioinspiration and Biomimetics* 2017;12:1–16.

[23] Khairi, T., Khairuddin, A., Lionheart, W. R. B. Some Properties of the First Order Polarization Tensor for 3-D Domains 2013;29:1–18.

[24] Capdeboscq, Y., Karrman, A. B., Nedelec, J. C. Numerical computation of approximate generalized polarization tensors. *Appl Anal* 2012;91:1189–203.

[25] Khairi, T., Khairuddin, A., Lionheart, W. R. B. Computing the First Order Polarization Tensor : Welcome BEM ++ ! *Menemui Mat* 2013;35:15–20.

[26] Lu, M., Zhao, Q., Hu, P., Yin, W., Peyton, A. J. Prediction of the asymptotical magnetic polarization tensors for cylindrical samples using the boundary element method. *SAS 2015 - 2015 IEEE Sensors Appl Symp Proc* 2015:1–4.

[27] Schoberl, J. Netgen - 4.x. RWTH Aachen Univ Ger 2009:39.

[28] Khairuddin, T. K. A., Lionheart W. R.B. Numerical Comparisons for the Approximated First Order Polarization, Tensor for Ellipsoids. *Appl Math Comput Intelligence* 2015;4:341–54.